1521-009X/42/9/1498–1507$25.00
Drug Metabolism and Disposition

http://dx.doi.org/10.1124/dmd.114.057836
Drug Metab Dispos 42:1498–1507, September 2014

Characterization of Arachidonic Acid Metabolism by Rat Cytochrome P450 Enzymes: The Involvement of CYP1As

Ahmed A. El-Sherbeni and Ayman O.S. El-Kadi

Faculty of Pharmacy and Pharmaceutical Sciences, University of Alberta, Edmonton, Alberta, Canada

Received February 26, 2014; accepted June 26, 2014

ABSTRACT

Cytochrome P450 (P450) enzymes mediate arachidonic acid (AA) oxidation to several biologically active metabolites. Our aims in this study were to characterize AA metabolism by different recombinant rat P450 enzymes and to identify new targets for modulating P450-AA metabolism in vivo. A liquid chromatography-mass spectrometry method was developed and validated for the simultaneous measurements of AA and 15 of its P450 metabolites. CYP1A1, CYP1A2, CYP2B1, CYP2C6, and CYP2C11 were found to metabolize AA with high catalytic activity, and CYP2A1, CYP2C13, CYP2D1, CYP2E1, and CYP3A1 had lower activity. CYP1A1 and CYP1A2 produced ω-1→4 hydroxyeicosatetraenoic acids (HETEs) as 88.7 and 62.7%, respectively, of the total metabolites formed. CYP2C11 produced epoxyeicosatrienoic acids (EETs) as 61.3%, and CYP2C6 produced midchain HETEs and EETs as 48.3 and 29.4%, respectively, of the total metabolites formed. The formation of CYP1A1, CYP1A2, CYP2C6, and CYP2C11 major metabolites followed an atypical kinetic profile of substrate inhibition. CYP1As inhibition by α-naphthoflavone or anti-CYP1As antibodies significantly reduced ω-1→4 HETE formation in the lungs and liver, whereas CYP1As induction by 3-methylcholanthrene resulted in a significant increase in ω-1→4 HETEs formation in the heart, lungs, kidney, and livers by 370, 646, 532, and 848%, respectively. In conclusion, our results suggest that CYP1As and CYP2Cs are major players in the metabolism of AA. The significant contribution of CYP1As to AA metabolism and their strong inducibility suggest their possible use as targets for the prevention and treatment of several diseases.

Introduction

Arachidonic acid (AA) is an ω-6 polyunsaturated fatty acid that is found incorporated in cellular membranes; therefore, it is abundant in all body organs. In normal conditions, AA is kept esterified to the sn-2 position of glycerophospholipids; its unesterified form is released at a lower rate (Imig, 2012). In response to stimuli, phospholipase A_2 releases the unesterified AA to be metabolized into biologically active metabolites, termed eicosanoids. AA metabolism to eicosanoids is mediated by one of three groups of enzymes: cyclooxygenases, lipoxygenases, or cytochrome P450 (P450). It has been reported that P450 enzymes catalyze oxygen insertion to give 15 different epoxy- and hydroxy–AA-metabolites (Fig. 1) (Capdevila et al., 2000). Epoxy-metabolites comprise four epoxyeicosatrienoic acids (EETs), namely, 5,6-, 8,9-, 11,12-, and 14,15-EET (Fig. 1) (Capdevila, 2007). Whereas hydroxy-metabolites can be divided into two main groups: 1) the midchain hydroxyeicosatetraenoic acids (mHETEs), namely, 5-, 8-, 9-, 11-, 12-, and 15-HETE (Fig. 1), and 2) the terminal/subterminal hydroxyeicosatetraenoic acids (ω/ω-1→4 HETEs), namely, 16-, 17-, 18-, 19-, and 20-HETE (Fig. 1) (Capdevila, 2007).

Despite P450-mediated AA metabolism being first reported about 30 years ago, P450-AA metabolites have only recently garnered much attention (Roman, 2002). The significant and multifaceted roles of P450-AA metabolites in the regulation of several biologic functions have now been recognized. EETs are reported to have vasodilatory, antiplatelet, anti-inflammatory, antinociceptive, fibrinolytic, vascular smooth muscle antimigratory, and angiogenic activities (Roman et al., 2000; Imig, 2012). On the other hand, 20-HETE exhibits vasoconstrictor, proinflammatory, and profibrotic activities (Zou et al., 1996; Stec et al., 2007). ω-1→4 HETEs, in addition to their suggested role as the endogenous 20-HETE antagonists, induce renal vasodilation and inhibit neutrophil adhesion (Alonso-Galicia et al., 1999; Bednar et al., 2000; Zhang et al., 2005). mHETEs induce cellular hypertrophy, inflammation, and fibrosis (Reddy et al., 2002; Kayama et al., 2009). Therefore, collectively, EETs and ω-1→4 HETEs exhibit several beneficial effects, whereas 20-HETE and mHETEs exhibit several harmful effects on biologic systems.

It has been reported that alterations in P450-AA metabolites levels are associated with several pathologic conditions (Roman, 2002; El-Sherbeni et al., 2013; Morisseau, 2013). Attributing these metabolic alterations to certain P450 enzyme(s) can provide novel protein targets for the prevention and treatment of several diseases, which requires characterizing AA metabolism by individual P450 enzymes. In this context, only a few studies have compared AA metabolism by P450 under the same experimental conditions. Furthermore, almost all of these studies were limited to human P450 enzymes (Capdevila et al., 2000; Imig, 2012). Also, previously published studies on P450-mediated AA metabolism focused mainly on EETs and 20-HETE; as a result, mHETEs and ω-1→4 HETEs have been largely ignored, mainly as the result of the lack of sophisticated methods for the simultaneous measurement of mHETEs and ω-1→4 HETEs along with EETs and 20-HETE

This work was supported by a grant from the Canadian Institutes of Health Research (CIHR) [Grant MOP 106665]. A.A.E.-S. is the recipient of an Egyptian Government Scholarship.

dx.doi.org/10.1124/dmd.114.057836.

ABBREVIATIONS: AA, arachidonic acid; α-NF, α-naphthoflavone; EET, epoxyeicosatrienoic acid; EROD, 7-ethoxyresorufin; HETE, hydroxyeicosatetraenoic acid; mHETE, midchain hydroxyeicosatetraenoic acid; ω/ω-1→4 HETE, terminal/subterminal hydroxyeicosatetraenoic acid; 3-MC, 3-methylcholanthrene; MROD, 7-methoxyresorufin; P450, cytochrome P450; SD, Sprague-Dawley rats.

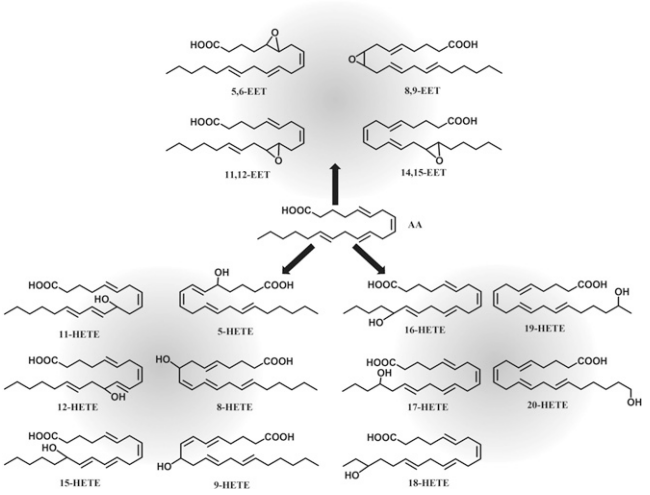

Fig. 1. P450-derived AA metabolites: mHETEs, ω/ω-1→4 HETEs and EETs.

(Blewett et al., 2008). The fact that the alterations of P450-AA metabolites levels are almost exclusively studied in animals, especially rats, mandates the study of animal P450 enzymes as well, keeping in mind that the determination and consequent pharmacological modulation of the involved enzymes need to be tested in animals before proceeding to clinical trials.

In the current study, we performed a comparative study to characterize the metabolism of AA by rat P450 enzymes to EETs, mHETEs, and ω/ω-1→4 HETEs. The following were our aims: 1) to develop and validate a simple liquid chromatography-mass spectrometry method for the simultaneous determination of the 15 P450-AA metabolites, 2) to determine the AA-metabolizing activity and metabolic profile of rat recombinant P450 enzymes, 3) to determine the kinetic profile of rat P450 enzymes of the highest AA-metabolizing activity, and 4) to identify new targets for modulating P450-AA metabolites in vivo.

Materials and Methods

Butylated hydroxytoluene, formic acid, NADPH, triethylamine, α-naphthoflavone (α-NF), and 3-methylcholanthrene (3-MC) were purchased from Sigma-Aldrich (St. Louis, MO). AA and AA metabolite standards 5,6-, 8,9-, 11,12- and 14,15-EET, and 5-, 8-, 9-, 11-, 12-, 15-, 16-, 17-, 18-, 19- and 20-HETE, as well as the deuterated AA, 14,15-EET, and 15-HETE (internal standards) were purchased from Cayman Chemical (Ann Arbor, MI). High-performance liquid chromatography–grade acetonitrile, methanol, isopropanol, water, and ethyl acetate were purchased from EM Scientific (Gibbstawn, NJ). Potassium dihydrogen phosphate, dipotassium hydrogen phosphate, and magnesium chloride hexahydrate were obtained from BDH Chemicals (Toronto, ON, Canada). Rat CYP1A1-, CYP1A2-, CYP2A1-, CYP2B1-, CYP2C6-, CYP2C11-, CYP2C13-, CYP2D1-, CYP2E1-, and CYP3A1-containing cell microsomes supplemented with NADPH-P450 reductase (Supersomes) were obtained from Gentest (Woburn, MA); cytochrome b_5 and NADPH-P450 reductase were from Oxford Biomedical Research (Oxford, MI). Mouse anti-rat CYP1A1 and goat anti-rat glyceraldehyde 3-phosphate dehydrogenase were purchased from Santa Cruz Biotechnology (Santa Cruz, CA). Other chemicals were purchased from Fisher Scientific (Toronto, ON, Canada).

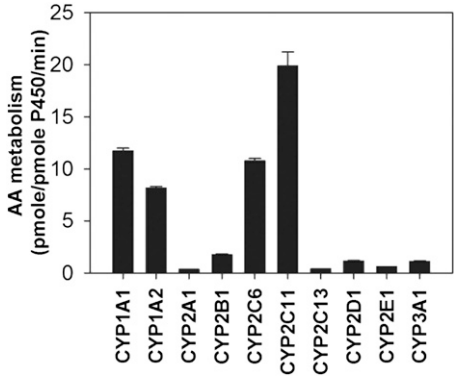

Fig. 2. AA-metabolizing activity of rat recombinant P450 enzymes. P450 enzymes (50–100 pmol/ml) were incubated with AA (75 μM) for 15–25 minutes as described under *Materials and Methods*. AA was measured by liquid chromatography-electrospray ionization-mass spectrometry. Results are presented as mean percentage and S.E. and are based on at least three individual experiments.

Animals and Treatment. All rats were maintained and used in accordance with the animal protocol approved by the University of Alberta Health Sciences Animal Policy and Welfare Committee, Edmonton, AB, Canada. Male Sprague-Dawley (SD) rats (Charles River Canada, St. Constant, QC, Canada) weighing 400–500 g were used. All animals were allowed free access to food and water. Four rats were injected intraperitoneally with 20 mg/kg 3-MC daily for 3 days ($n = 4$). Weight-matched controls received the same volume of corn oil ($n = 4$). Also, five untreated SD rats were used for the isolation of heart, lung, kidney, and liver microsomes.

Microsomal Preparation. Animals were euthanized under isoflurane anesthesia. Heart, lung, kidney, and liver were excised, immediately frozen in liquid nitrogen, and stored at −80°C until microsomal preparation. Microsomal fractions from heart, lung, kidney, and liver of the SD rats were separated by differential centrifugation of homogenized tissues as described previously (Barakat et al., 2001). Briefly, organs were washed in ice-cold potassium chloride (1.15%, w/v). Subsequently, they were cut into pieces and homogenized in ice-cold 0.25 M sucrose solution (17%, w/v). For untreated rats, homogenates of each organ were pooled together (c.f. other rat groups). Thereafter, microsomal fractions were separated by differential ultracentrifugation. The final pellet was resuspended in cold sucrose and stored at −80°C. The microsomal protein concentration was determined by the Lowry method using bovine serum albumin as a standard (Lowry et al., 1951).

Apparatus and Chromatographic Conditions. AA and P450-AA metabolites were analyzed simultaneously using liquid chromatography-electrospray ionization-mass spectrometry (Waters Micromass ZQ 4000 spectrometer; Waters Corporation, Milford, MA). The mass spectrometer was run in negative ionization mode with single ion monitoring. The nebulizer gas was acquired from an in-house high-purity nitrogen source. The temperature of the source was set at 150°C, and the capillary and cone voltage were 3.51 kV and 25 V, respectively. A gradient separation was performed on a reverse-phase C18 column (Alltima HP, 250 × 2.1 mm; GRACE Davison, Lokeren, Belgium) at 35°C. Mobile phase A consisted of water with 0.01% formic acid and 0.005% triethylamine (v/v), whereas mobile phase B consisted of 8% methanol, 8% isopropanol, and 84% acetonitrile with 0.01% formic acid and 0.005% triethylamine (v/v). Samples were subjected to linear gradient elution at a flow rate of 200 μl/min, as follows: 60 to 48% in 4 minutes, held isocratically at 48% for 24 minutes, 48 to 35% in 11 minutes, 35 to 0% in 11 minutes, and finally held isocratically at 0% for 7 minutes of mobile phase A.

Method Validation. The linearity of the method was evaluated in the range of 0.014 to 1370 μg/ml for AA (10 concentrations) and 0.005 to 4.5 μg/ml for AA metabolites (10 concentrations). Calibration curves constructed on three separate days were analyzed to evaluate the linearity. Accuracy and precision were determined using quality-control samples at four levels in the range of expected concentrations in incubates, 0.14, 1.37, 13.7, and 68.5 μg/ml for AA and 0.005, 0.045, 0.45, and 4.5 μg/ml for AA metabolites. Each quality-control sample (10 μl) was injected in triplicate on three different days to permit an assessment of intraday and interday accuracy and precision. Accuracy was determined by the calculating the concentration of each quality-control sample based on the calibration curve equations. Bias was assessed by calculating percentage of error [%error = $(C_{\text{calculated}} - C_{\text{nominal}})/C_{\text{nominal}} \times 100$] for all injections at each level analyzed. Precision was assessed by calculating the coefficient of variation (%CV = S.D./mean × 100) for all injections at each level analyzed.

Arachidonic Acid Metabolism. P450-mediated AA metabolism was characterized in an incubation mixture (200 μl) containing 3 mM magnesium chloride hexahydrate, NADPH-P450 reductase, cytochrome b_5, P450, and AA in

100 mM potassium phosphate buffer (pH 7.4). Preliminary incubations were performed to ensure that the formation of AA metabolites was linear with respect to incubation time and protein content under assay conditions: 50 pmol/ml of CYP1A1, CYP1A2, CYP2C6, CYP2C11, or CYP2C13 or 100 pmol/ml of CYP2A1, CYP2B1, CYP2D1, CYP2E1, or CYP3A1 was incubated with AA (75 μM) for 15–25 minutes according to the tested P450. For untreated, 3-MC–treated, and corn-oil–treated rats, 0.5 mg/ml of microsomal protein separated from the heart, lungs, kidneys, or liver was incubated with AA (75 μM) for 30 minutes. For the kinetic experiments, AA concentrations varied from 15 to 320 μM and incubated for 15 minutes with 50 pmol/ml of CYP1A1, CYP1A2, CYP2C6, and CYP2C11. Incubations were conducted at 37°C in a shaking water bath (90 rpm) after a 5-minute pre-equilibration period. The reaction was initiated by the addition of the cofactor NADPH (final concentration, 2 mM) and terminated by the addition of 600 μl ice-cold acetonitrile containing 0.01% formic acid and 0.001% butylated hydroxytoluene. The incubation mixtures were double-extracted with 1 ml of ethyl acetate; thereafter, the organic extracts were combined, evaporated to dryness, and reconstituted in 50 μl of acetonitrile containing 0.01% formic acid. Three standard samples were prepared by spiking protein preparation with known amounts of tested compounds, as well as internal standards. The final concentrations of the tested compounds were 0.01, 0.1, and 1 μg/ml for AA metabolites and 0.24, 2.4, and 24 μg/ml for AA, whereas the final concentration of internal standards was 0.25 μg/ml. Standard samples were subjected to the same extraction procedure as test samples to be analyzed at the beginning and at the end of the run. The concentrations of the AA metabolites were determined from standard curves using analyte to internal standard peak area (response ratio).

Measuring CYP1A1 and CYP1A2 Activity. The *O*-dealkylation of 7-ethoxyresorufin (EROD) or 7-methoxyresorufin (MROD) by CYP1A1 or CYP1A2, respectively, was measured in incubation buffer consisting of 3 mM magnesium chloride hexahydrate in 100 mM potassium phosphate buffer (pH 7.4). In a total volume of 200 μl, microsomal protein of rat heart (1 mg/ml), lung (1 mg/ml), kidney (1 mg/ml), or liver (0.25 mg/ml) was incubated with 0, 10, 20, 40, 80, 160, or 250 nM of α-NF for 10 minutes on ice. Then, 0.4 nmol of EROD or MROD was added, followed by the addition of NADPH to initiate the reaction. Fluorescence associated with resorufin formation was measured every 2 minutes (excitation and emission wavelengths of 535 and 585 nm) for 30 minutes at 37°C using a BioTek Synergy H1 Hybrid Reader (BioTek Instruments, Winooski, VT). The initial rate of product formation in each well was determined by linear regression of fluorescence-time data.

Inhibition of CYP1A-Mediated AA Metabolism in the Heart, Lungs, Kidneys, and Liver. To determine the contribution of CYP1As to AA metabolism, the effect of CYP1A inhibition on P450-mediated AA metabolism was studied in microsomal fractions of the heart, lungs, kidneys, and liver. Chemical inhibition by selective CYP1A inhibitor (α-NF) and immunoinhibition by selective anti-CYP1As antibodies were used. For chemical inhibition, 100 μg of microsomal protein was incubated with 0, 40, and 160 nM of α-NF for 10 minutes on ice (all samples contained a fixed concentration of 0.1% dimethylsulfoxide). AA (75 μM) was added, and the reaction was initiated by the addition of NADPH and terminated by the addition of acetonitrile as described. For immunoinhibition, 30 μg of microsomal protein was added to 20 μg of anti-CYP1As or anti–glyceraldehyde 3-phosphate dehydrogenase antibodies (nonspecific rat antibody) and kept for 30 minutes on ice. Then AA (75 μM) was added, and the reaction was initiated by the addition of NADPH and terminated after 60 minutes by the addition of acetonitrile as described herein. The incubation mixtures were double-extracted with 1 ml of ethyl acetate; thereafter, the organic extracts were combined, evaporated to dryness, and reconstituted in 50 μl of acetonitrile containing 0.01% formic acid.

Data Analysis. To determine the kinetics of P450-mediated AA metabolism, nonlinear regression was performed using GraphPad Prism (version 5.01; GraphPad Software, La Jolla, CA). The rate of AA metabolite formation versus AA concentration data was fitted to several models of enzyme kinetics: Michaelis-Menten model (eq. 1) and its modified version to include homotropic cooperativity, Hill equation (eq. 2), were used (Kramer and Tracy, 2008). It is estimated that in about 20% of enzymatic reactions, enzyme activity is inhibited by the presence of excess substrate. Therefore, substrate inhibition models, Haldane's equation (eq. 3), and its modified version to include homotropic cooperativity (eq. 4) were also used (LiCata and Allewell, 1997; Kapelyukh et al., 2008; Reed et al., 2010):

$$Rate\ of\ formation = \frac{V_{max} \times [AA]}{K_m + [AA]} \quad (1)$$

$$Rate\ of\ formation = \frac{V_{max} \times [AA]^h}{K_m^h + [AA]^h} \quad (2)$$

$$Rate\ of\ formation = \frac{V_{max} \times [AA]}{K_m + [AA] + \frac{[AA]^2}{K_{si}}} \quad (3)$$

$$Rate\ of\ formation = \frac{V_{max} \times [AA]^h}{K_m^h + [AA]^h + \frac{[AA]^{2h}}{K_{si}^h}} \quad (4)$$

where V_{max} is the maximal rate of formation, K_m is the affinity constant, [AA] is the concentration of AA, h is Hill coefficient, and K_{si} is the inhibition constant. The optimal enzyme kinetics model was determined by the Akaike information criterion as a measure of the goodness of fit.

Statistical Analysis. Data are presented as mean ± S.E. Student's *t*-test or one-way analysis of variance, followed by a Tukey's post hoc test, was used. A result was considered statistically significant where $P < 0.05$.

Results

Liquid Chromatography-Electrospray Ionization-Mass Spectrometry Method Development and Validation. Previous reverse-phase liquid chromatography methods used gradient elution of acidified acetonitrile or methanol with water for separating P450-AA metabolites. However, the coelution of mHETEs, in addition to the coelution of ω/ω-1→4 HETEs, was the common drawback for all these methods (Choudhary et al., 2004). Therefore, additional normal-phase liquid or gas chromatographic methods were used to achieve the complete resolution of P450-AA by reanalyzing the eluate collected from an initial reverse-phase separation (Carroll et al., 1997; Kiss et al., 2000; Schwarz et al., 2004). Tandem mass spectrometry detection could be another way to achieve successful one-step resolution of mHETE, as well as ω/ω-1→4 HETEs (Norris et al., 2011; Edpuganti and Mehvar, 2013). Therefore, we aimed to develop a reverse-phase liquid chromatographic method for one-step, simultaneous separation of all P450-AA metabolites without the expensive tandem mass spectrometry equipment or the complications of normal-phase chromatography.

We found that methanol-based gradient elution gave very poor resolution for 16-, 17-, 18-, 19-, and 20-HETE and 8-, 9-, 11-, and 12-HETE. For acetonitrile-based elution, it could not resolve 8-HETE from 12-HETE and 16-HETE from 17-HETE. Adding isopropanol to either methanol or acetonitrile led to the coelution of 5-HETE with 14 and 15-EET and 18-HETE with 20-HETE. Resolution of AA and its 15 P450-AA metabolites was achieved by adding 16% of equivolume mixture of methanol and isopropanol to acetonitrile as the organic mobile phase. With respect to P450-AA metabolites, the retention time and the linear range that extended over 4 orders of magnitude are shown in Table 1. Three internal standards, AA-d8 for AA quantification, 14,15-EET-d11 for EETs quantification, and 15-HETE-d8 for HETEs quantification, were monitored at m/z = 311, 330, and 327, respectively, and their retention times were 53.5, 46, and 37 minutes, respectively. The lower limit of quantitation of the assay based on the mean %error and %CV results was in the range of 0.05–0.45 ng (Table 1). The intraday and interday precision determined at all concentration levels did not exceed 15% of the %CV (Table 2). With respect to intraday and interday accuracy (Table 2), the mean %error did not exceed 15% for all concentration levels.

TABLE 1

The retention times (R_t), ions monitored, sensitivity, and linearity results of cytochrome P450-arachidonic acid metabolites analysis

Compound	SIM	R_t	Linear Range	r^2	LOQ
	m/z	*min*	*ng*		*ng*
AA	303	53.5	1.4–244	0.99	1.4
5-HETE	319	45.5	0.45–45	0.99	0.45
8-HETE	319	42.5	0.05–45	0.99	0.05
9-HETE	319	43.5	0.05–45	0.99	0.05
11-HETE	319	40.5	0.05–45	0.99	0.05
12-HETE	319	42	0.05–45	0.99	0.05
15-HETE	319	38	0.45–45	0.99	0.45
16-HETE	319	33	0.45–45	0.99	0.45
17-HETE	319	32	0.45–45	0.99	0.45
18-HETE	319	30.5	0.05–45	0.99	0.05
19-HETE	319	28	0.45–45	0.99	0.45
20-HETE	319	29.5	0.45–45	0.99	0.45
5,6-EET	319	49.5	0.45–45	0.99	0.45
8,9-EET	319	48.5	0.45–45	0.99	0.45
11,12-EET	319	48	0.05–45	0.99	0.05
14,15-EET	319	46.5	0.05–45	0.99	0.05

LOQ, lower outer quadrant; SIM, Selected ion monitored.

Determination of AA-Metabolizing Activity and Metabolic Profile of P450 Enzymes. Ten rat recombinant P450 enzymes were included in our experiments, selected from different families and subfamilies to get a good idea about the differences in AA-metabolizing activity among rat P450 enzymes. No NADPH-independent formation of AA metabolites was mediated by preparation of Supersomes. Also, there was no formation of AA metabolites mediated by NADPH-P450 reductase or cytochrome b_5. With the addition of NADPH, all the tested P450 enzymes were able to metabolize AA but with substantial differences in their rates. Intracellular concentration of the unesterified AA is widely believed to be in the micromolar range, based on reports where the total concentration of unesterified AA has been determined in different tissues. For example, whereas the unesterified form of AA is in the nanomolar range in blood (Brash, 2001), its concentration has been reported to be 13–44 μM in umbilical cord and intervillous space (Benassayag et al., 1997), 18.9 μg/g (approximately equivalent to 60 μM) in skin (Hammarstrom et al., 1975), and 75 μg/g (approximately equivalent to 250 μM) in liver (Edpuganti and Mehvar, 2013). Therefore, 50–100 μM of AA was used in several published studies performed in AA-P450 incubation experiments (Xu et al., 2004; Imaoka et al., 2005). Therefore, 75 μM of AA was used to reflect the in vivo situation. CYP2C11 metabolized AA with the highest rate (19.9 pmol/pmol P450 per minutes), whereas CYP2A1 had the lowest rate (0.35 pmol/pmol P450 per minute) (Fig. 2). Interestingly, CYP1A1, CYP1A2, and CYP2C6, which have largely been ignored in P450-AA studies, were among the P450 of the highest activity (Fig. 2). In contrast, CYP2A1, CYP2B1, and CYP2E1, which are the focus of P450-AA studies, had relatively lower activity (Fig. 2).

With respect to P450 metabolic profile, all the tested P450 enzymes preferentially mediated AA hydroxylation more than olefin epoxygenation, except CYP2C11 (Figs. 3 and 4). Interestingly, CYP1A1 and CYP1A2 produced mainly ω-1→4 HETEs by 88.7 and 62.7%,

TABLE 2

Precision and accuracy results of representative cytochrome P450-arachidonic acid metabolites (n = 3)

Compound	Nominal conc.	%CV		%Error	
		Intraday	Interday	Intraday	Interday
	μg/ml				
AA	0.14	1.22	10.40	−11.25	3.67
	1.37	1.82	7.56	−19.52	−7.16
	13.7	2.81	0.56	1.53	−7.05
	68.5	0.97	10.67	14.89	−9.59
15-HETE	0.005	2.45	4.53	11.38	24.27
	0.045	1.75	3.29	−6.91	2.25
	0.45	1.02	3.75	10.61	1.70
	4.5	0.75	2.89	9.03	0.06
18-HETE	0.005	15.66	10.30	−0.02	16.19
	0.045	2.11	1.20	−11.15	4.88
	0.45	2.19	1.70	5.09	4.41
	4.5	1.80	5.01	0.02	0.24
8,9-EET	0.005	3.87	1.22	−3.18	22.91
	0.045	5.02	7.94	−9.53	9.03
	0.45	2.40	5.02	3.92	5.19
	4.5	2.30	5.10	0.04	0.18

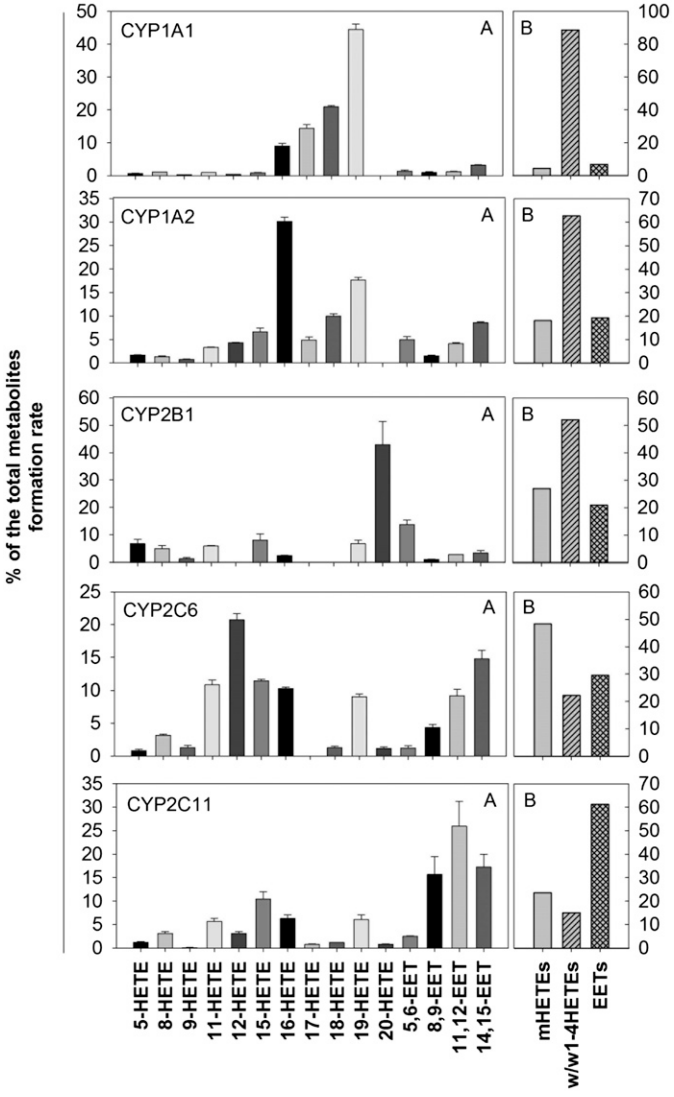

Fig. 3. The metabolic profile and regioselectivity of AA metabolism by CYP1A1, CYP1A2, CYP2B1, CYP2C6, and CYP2C11. P450 enzymes (50–100 pmol/ml) were incubated with AA (75 μM) for 15–25 minutes as described under *Materials and Methods*. AA metabolites were measured by liquid chromatography-electrospray ionization-mass spectrometry. (A) The percentage of each AA metabolite to the total metabolite formation. (B) Percentage of total mHETEs, ω/ω-1 HETEs, and EETs to the total metabolite formation. Results are presented as mean percentage and S.E. and are based on at least three individual experiments.

respectively (Fig. 3). For CYP2C6, the major metabolites were mHETEs (48.3%) and EETs (29.4%) (Fig. 3). Although for CYP2C11, EETs represented 61.3% of the total P450-AA metabolites formed, whereas mHETE and ω/ω-1→4 HETEs represented 23.6 and 15.1%, respectively (Fig. 3). Moreover, ω/ω-1→4 HETEs were the major metabolites for CYP2A1, CYP2B1, and CYP2E1 as 56.1, 52.1, and 68.7% of the total metabolites formed, respectively (Fig. 4), whereas mHETEs were the predominant metabolites for CYP2C13, CYP2D1, and CYP3A1 as 45, 47.3, and 81.8% of the total metabolites formed (Fig. 4). Also, P450 enzymes exhibited regioselective oxidation of AA. For CYP1A1, it preferentially oxidized AA to produce 19-HETE, whereas CYP1A2 produced mainly 16-HETE (Fig. 3). The main epoxy-metabolite for CYP2C11 and CYP2C6 were 11,12- and 14,15-EET, respectively (Fig. 3).

Determination of the Kinetic Profile of CYP1A1-, CYP1A2-, CYP2C6-, and CYP2C11-Mediated AA Metabolism. The high activity toward AA metabolism showed by CYP1A1, CYP1A2, CYP2C6, and CYP2C11 implies the predominant role of these P450 in AA metabolism in vivo. Therefore, the kinetic profile of CYP1A1, CYP1A2, CYP2C6, and CYP2C11 was determined. The rate of formation of P450-AA metabolites was measured at varied concentration of AA. An inhibition in P450 activity was observed by the excess addition of AA for all the tested P450 enzymes, indicating substrate inhibition kinetics. The model that demonstrated the best fit was eq. 4. The equation describes substrate inhibition in addition to homotropic cooperativity, indicating binding of more than one AA molecule to the tested enzymes. A shared value for K_{si} among the metabolites for each P450 enzymes was assumed; the K_{si} values were 132, 121, 142, and 82.9 μM for CYP1A1, CYP1A2, CYP2C6, and CYP2C11, respectively. Kinetic parameter mean values are shown for the four major metabolites of each enzyme (Table 3). The K_m values ranged from 40 to 52 μM for the major metabolites of CYP1A1 and from 10 to 11 μM for the major metabolites of CYP1A2. On the other hand, K_m values ranged from 13 to 36 μM for the major metabolites of CYP2C6 and from 60 to 90 μM for the major metabolites of CYP2C11.

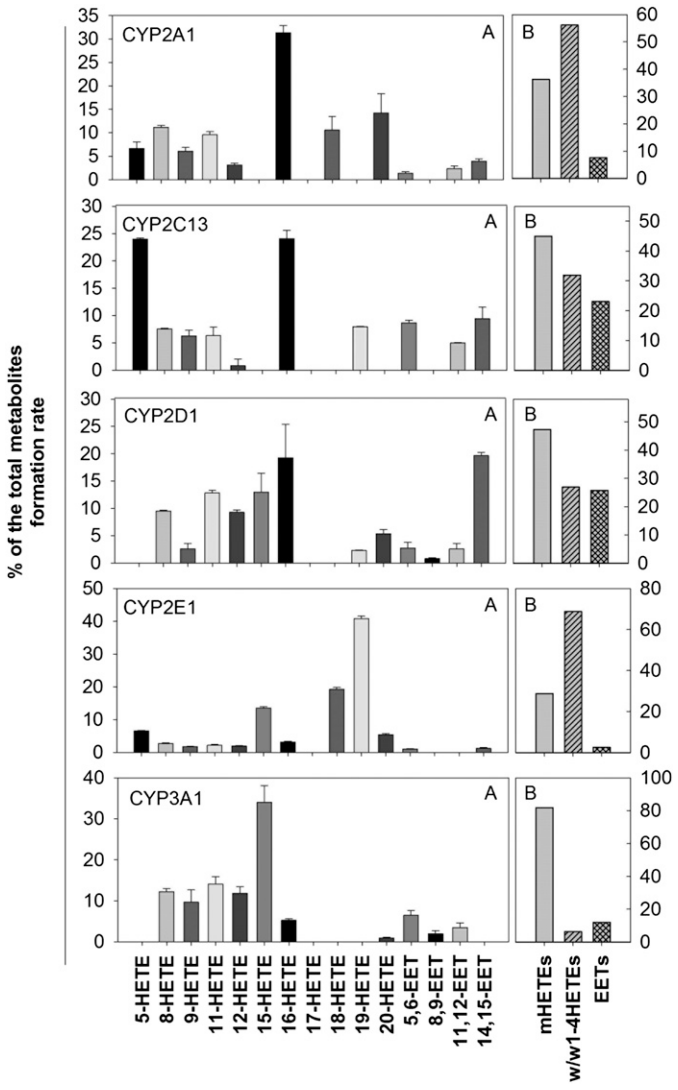

Fig. 4. The metabolic profile and regioselectivity of AA metabolism by CYP2A1, CYP2C13, CYP2D1, CYP2E1, and CYP3A1. P450 enzymes (50–100 pmol/ml) were incubated with AA (75 μM) for 15–25 minutes as described under *Materials and Methods*. AA metabolites were measured by liquid chromatography-electrospray ionization-mass spectrometry. (A) Percentage of each AA metabolite to the total metabolite formation. (B) Percentage of total mHETEs, ω/ω-1 HETEs, and EETs to the total metabolite formation. Results are presented as mean percentage, and S.E. and are based on at least three individual experiments.

Determination of AA Metabolic Profile of Heart, Lung, Kidney, and Liver Microsomes. We showed that individual rat recombinant P450 enzymes are able to mediate oxidation of AA to several EETs and HETEs. To determine whether this also occurs in the in vivo condition of competing coexpressed P450 enzymes, we studied AA metabolism by the heart, lungs, kidneys, and liver microsomes. The formation of the three groups of P450-AA metabolites, mHETEs, ω/ω-1→4 HETEs, and EETs were mediated by the heart, lung, kidney, and liver microsomes (Fig. 5; Table 4). EETs were the major metabolites formed, of which 11,12-EET was the most abundant, for the heart, kidney, and liver (Fig. 5; Table 4), whereas for the lungs, mHETEs were the major metabolites, of which 15-HETE was the most abundant (Fig. 5; Table 4). As expected, the liver exhibited the highest AA-metabolizing activity because of its high P450 content, followed by the kidneys, compared with the heart and lungs, which exhibited comparably lower activity (Table 4). For ω-1→4 HETEs, which are the major metabolites for CYP1A1 and CYP1A2, the liver had the highest activity and then the kidneys, followed by the lungs and heart (Table 4).

Determination of the Contribution of CYP1A1 and CYP1A2 to AA Metabolism in Heart, Lung, Kidney, and Liver. Our findings showed that CYP1A1 and CYP1A2 have high AA-metabolizing activity compared with other rat P450s. However, the contributions of CYP1A1 and CYP1A2 to tissue-mediated AA metabolism have never been studied, and the role of CYP1A1 and CYP1A2 in AA metabolism has been underestimated. To determine the contribution of these two enzymes to AA metabolism in rat organs, we determined 1) the effect of CYP1As inhibition by selective CYP1A chemical inhibitors, α-NF, and anti-CYP1As antibodies; and 2) the effect of CYP1A induction by an aryl hydrocarbon receptor agonist (3-MC) on the metabolism of AA mediated by microsomal fractions of the heart, lungs, kidneys, and liver. Combining the results of these three experiments would allow determination of the specific contribution of CYP1As to AA metabolism in different rat organs.

With respect to CYP1As chemical inhibition, 6 α-NF concentrations were tested for CYP1A inhibition by EROD and MROD assays. Consequently, 40 and 160 nM of α-NF, which caused a 28 and 95% inhibition of EROD activity, respectively, and 41 and 63% inhibitions of MROD activity, respectively, were tested for their effect on AA metabolism. α-NF at 40 nM significantly inhibited liver-mediated formation of 16- and 19-HETE by 24.3 and 25.9%, respectively (Table 5), whereas α-NF at 160 nM significantly inhibited lung-mediated formation of 16- and 19-HETE by 37.5 and 80.2%, respectively, as well as

TABLE 3

Enzyme kinetic parameters for the formation of major metabolites of CYP1A1, CYP1A2, CYP2C6, and CYP2C11

Data are the mean and S.E.E. (standard error of estimate), V_{max} (in picomoles per picomoles of P450 per minute), K_m and K_{si} (in micromolars), and h were determined as per (eq. 4). Cl_{int} [intrinsic clearance (in microliters per minute per picomoles P450)] was calculated. as V_{max}/K_m.

Compound		V_{max}	K_m	K_{si}	h	Cl_{int}	R^2
CYP1A1	16-HETE	1.79 ± 0.36	41.6 ± 9.32	132 ± 15	2.46 ± 0.61	0.04	0.88
	17-HETE	2.39 ± 0.45	51.6 ± 10.5	132 ± 15	2.30 ± 0.44	0.05	0.96
	18-HETE	3.77 ± 0.60	48.3 ± 7.32	132 ± 15	2.37 ± 0.32	0.08	0.96
	19-HETE	7.75 ± 1.04	39.5 ± 4.77	132 ± 15	2.27 ± 0.22	0.20	0.96
CYP1A2	16-HETE	2.18 ± 0.13	10.1 ± 0.82	121 ± 5.33	2.71 ± 0.44	0.22	0.98
	17-HETE	0.44 ± 0.14	11.3 ± 6.53	121 ± 5.33	2.00 ± 0.55	0.04	0.99
	18-HETE	0.73 ± 0.11	9.92 ± 2.31	121 ± 5.33	2.71 ± 1.41	0.07	0.98
	19-HETE	1.17 ± 0.11	9.76 ± 1.26	121 ± 5.33	3.00 ± 1.00	0.12	0.98
CYP2C6	12-HETE	2.65 ± 0.29	18.3 ± 2.84	142 ± 5.91	2.39 ± 0.55	0.14	0.96
	15-HETE	0.82 ± 0.13	13 ± 2.02	142 ± 5.91	5.40 ± 2.33	0.06	0.93
	11,12-EET	1.49 ± 0.40	35.9 ± 18.5	142 ± 5.91	1.44 ± 0.54	0.04	0.97
	14,15-EET	2.10 ± 0.39	31.9 ± 11.1	142 ± 5.91	1.46 ± 0.38	0.07	0.97
CYP2C11	5,6-EET	4.99 ± 1.26	90.2 ± 43.7	82.9 ± 5.05	1.33 ± 0.42	0.06	0.90
	8,9-EET	8.36 ± 1.25	65.6 ± 10.6	82.9 ± 5.05	2.13 ± 0.29	0.13	0.97
	11,12-EET	12 ± 1.38	60.1 ± 6.78	82.9 ± 5.05	2.18 ± 0.20	0.20	0.96
	14,15-EET	7.77 ± 1.14	62.3 ± 11.2	82.9 ± 5.05	1.89 ± 0.28	0.12	0.98

liver-mediated formation of 16- and 19-HETE by 43.6 and 52%, respectively (Table 5). In agreement with chemical inhibition results, immunoinhibition of CYP1A resulted in a significant decrease in lung-, kidney- and liver-mediated formation of 19-HETE by 83.9, 26.5, and 66.2%, respectively (Table 6). Also, liver-mediated formation of 16-HETE was also significantly decreased by 41.2% (Table 6). Inhibition of CYP1As resulted in more pronounced effects on liver-mediated AA metabolism, which included not only ω/ω-1→4 HETEs but also mHETEs and EETs formation (Table 6). The formation of 14,15-EET was significantly inhibited (15.8%) by α-NF, whereas formation of EETs was significantly inhibited (52% average) by anti-CYP1A antibodies. For mHETEs, 12-HETE was significantly inhibited (9.6%) by α-NF, whereas 8-, 11-, 12-, and 15-HETE formation was significantly inhibited (38% average) by anti-CYP1A antibodies (Table 6). For the heart, inhibition of CYP1As did not result in any significant alteration in AA metabolism, except inhibition of 11,12-EET formation (22.6%) by α-NF (Tables 5 and 6).

On the other hand, 3-day treatment of 3-MC led to a significant induction in CYP1A activities in all four organs compared with corn-oil–treated (control) group. In the heart, lungs, kidneys, and liver, CYP1A1 activity measured by EROD assay showed a 13,500, 2070, 1120, and 1160% induction, whereas CYP1A2 activity measured by MROD assay showed a 300, 310, 510, and 3600% induction, respectively, compared with control group (Fig. 6). This observed induction in CYP1As resulted in a significant increase in the formation of ω-1→4 HETEs for all four organs. The formation of 16-, 17-, 18-, and 19-HETE was significantly increased by 131, 183, 415, and 750%,

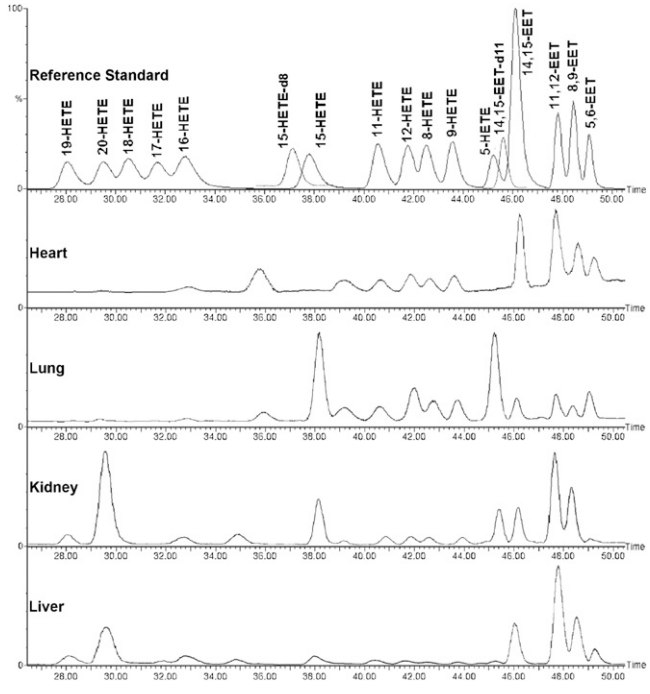

Fig. 5. AA metabolites formation mediated by rat heart, lung, kidney, and liver microsomes. The chromatograms of reference standard, heart, lung, kidney, and liver samples were determined by liquid chromatography-electrospray ionization-mass spectrometry using selected ion monitoring at m/z = 319 for AA metabolites and internal standards at m/z = 327 and 330 for 15-HETE-d8 and 14,15-EET-d11, respectively. Microsomal protein from the heart, lungs, kidneys, or liver (100 μg) was incubated with AA (75 μM) for 30 minutes as described in *Materials and Methods*.

TABLE 4

Formation rate of arachidonic acid metabolites mediated by rat heart, lung, kidney, and liver microsomal fractions

Compound	Formation Rate[a]			
	Heart	Lung	Kidney	Liver
	pmol/mg protein/min			
5-HETE	—	74.9 ± 6.69	75.6 ± 5.42	60.9 ± 2.67
8-HETE	6.28 ± 0.42	23.4 ± 1.61	27.5 ± 1.81	51.4 ± 2.93
9-HETE	5.34 ± 0.46	20.9 ± 1.22	21.4 ± 1.11	19.5 ± 1.38
11-HETE	6.40 ± 0.41	24.8 ± 2.39	24.9 ± 1.46	103 ± 7.97
12-HETE	7.15 ± 0.48	34.6 ± 2.21	24.3 ± 1.30	84.0 ± 6.98
15-HETE	—	81.3 ± 5.47	90.1 ± 5.33	202 ± 12.8
16-HETE	2.49 ± 0.23	2.47 ± 0.17	25.5 ± 1.44	234 ± 6.68
17-HETE	—	—	—	70.3 ± 1.79
18-HETE	—	—	—	—
19-HETE	0.1 ± 0.03	0.45 ± 0.02	20.0 ± 1.46	181 ± 6.96
20-HETE	0.49 ± 0.07	1.85 ± 0.11	258 ± 14.5	546 ± 29.4
5,6-EET	7.98 ± 0.86	19.1 ± 1.18	15.4 ± 1.68	256 ± 6.79
8,9-EET	11.8 ± 0.80	10.2 ± 0.57	126 ± 6.97	505 ± 31.8
11,12-EET	26.6 ± 1.04	20.5 ± 1.20	225 ± 15.6	883 ± 47.8
14,15-EET	22.6 ± 1.41	16.0 ± 1.27	86.8 ± 5.55	364 ± 35.8

[a]Data are the mean and S.E.M. based on at least three individual experiments; —, undetectable formation.

TABLE 5

Effect of CYP1A inhibitor α-naphthoflavone on arachidonic acid metabolism mediated by the rat heart, lung, kidney, and liver microsomal fractions

	% Inhibition[a]							
	Heart		Lung		Kidney		Liver	
	40 nM	160 nM	40 nM	160 nM	40 nM	160 nM	40 nM	160 nM
5-HETE	—	—	12.1	15.3	−4.02	−1.88	3.61	6.59
8-HETE	−3.29	7.26	−9.45	−14.1	−8.56	3.20	2.82	1.27
9-HETE	−0.19	12.5	12	16.1	−0.12	4.54	4.26	9.06
11-HETE	−12.8	3.7	−17	9.37	−14.8	−5.51	2.30	4.52
12-HETE	−9.01	1.01	28.7	9.51	−8.11	0.18	3.37	9.60*
15-HETE	—	—	25.6	18.6	−11.7	−4.65	1.74	7.54
16-HETE	−13.8	8.68	15.3	37.5*	−18	−21.3	24.3*	43.6*
17-HETE	—	—	—	—	—	—	—	—
18-HETE	—	—	—	—	—	—	—	—
19-HETE	−3.59	7.98	36.6	80.2*	21.8	−9.96	25.9*	52*
20-HETE	−20.3	15.8	10.3	18.2	−23.1	−7.51	1.83	7.93
5,6-EET	5.77	15.4	34.2	−4.82	−22.7	−23.4	1.29	8.63
8,9-EET	1.22	11.1	7.80	−10.1	−16.7	−7.45	9.00	9.23
11,12-EET	−2.63	22.6*	8.56	−5.18	−11.5	−4.64	7.56	7.81
14,15-EET	6.69	13.2	−27.6	7.00	−6.00	−5.32	5.43	15.75*

[a]Data are based on at least three individual experiments.
*Inhibition was significant at $P < 0.05$; —, non-applicable.

respectively, for the heart; 171, 1200, 364, and 844%, respectively, for the lungs; and 200, 404, 2570, and 213%, respectively, for the liver compared with the control group (Fig. 7). For kidneys, the formation rate of 17- and 18-HETE was significantly increased, by 1380 and 536%, compared with the control group (Fig. 7). Additionally, there was a 142% increase in 12-HETE formation and a 51 and 34% decrease in 11,12-EET and 20-HETE formation, respectively, in 3-MC–treated livers compared with control livers (Fig. 7).

Discussion

Recently, P450-derived AA metabolites have been reported to have numerous physiologic and pathologic effects. Therefore, pharmacologic modulation of P450-mediated AA metabolism has great potential for the treatment and control of several diseases and pathologic conditions. In this regard, performing a comparison between the AA-metabolizing activities of several P450 would provide important information. In the current study, a simple high-performance liquid chromatography method was developed and validated for determining the formation of mHETEs, ω/ω-1→4 HETEs, and EETs by P450 enzymes. We selected 10 recombinant rat P450 enzymes from three different families, including enzymes that have not been studied before, such as CYP2D1 and CYP3A1, to be characterized. The AA-metabolizing activities of these enzymes were measured, and the kinetic profiles of P450 enzymes of the highest activity were determined. One interesting finding was the high AA-metabolizing activity of CYP1A1 and CYP1A2; consequently, we determined the involvement of CYP1A1 and CYP1A2 in AA metabolism in the rat heart, lungs, kidneys, and liver.

TABLE 6

Effect of anti-CYP1A antibodies on arachidonic acid metabolism mediated by rat heart, lung, kidney, and liver microsomal fractions

Compound	% Inhibition[a]			
	Heart	Lung	Kidney	Liver
5-HETE	—	−5.35	−11.33	−15.57
8-HETE	−14.12	−14.34	5.73	30.88*
9-HETE	−17.12	−12.87	−0.30	13.79
11-HETE	−14.28	−17.20	5.17	41.65*
12-HETE	−13.99	−11.55	6.67	35.64*
15-HETE	—	−14.36	0.62	39.72*
16-HETE	−17.85	−5.15	7.52	41.20*
17-HETE	—	—	—	—
18-HETE	—	—	—	—
19-HETE	−5.63	83.98*	26.45*	66.24*
20-HETE	−7.79	14.00	12.01	15.36
5,6-EET	7.96	−11.66	−0.91	43.35*
8,9-EET	−15.53	−16.92	19.44	59.14*
11,12-EET	−12.17	−3.99	22.68	54.49*
14,15-EET	−17.54	−3.92	24.57	51.64*

[a]Data are based on at least three individual experiments.
*Inhibition was significant at $P < 0.05$; —, non-applicable.

Interestingly, P450 enzymes tested in the current study were able to metabolize AA, including CYP2C6, CYP2C13, CYP2D1, and CYP3A1, which have never been investigated before. In several previously published papers, CYP2C6 and CYP2C13 were considered as AA epoxygenases (Holla et al., 1999; Iliff et al., 2010). However, our results showed that CYP2C6, as well as CYP2C13, mediates mainly AA hydroxylation. Although CYP2C6, CYP2C11, and CYP2C13 are of the same subfamily, there was substantial variation in their AA-metabolizing activities; CYP2C6 and CYP2C11 were among the highest, whereas CYP2C13 was among the lowest. In agreement with our results, it has been reported that CYP2C11 is the main epoxygenase in rats (Imig, 2012). It mediates AA metabolism to EETs as about two-thirds of total metabolites, and its regioselectivity was in the order of 11,12-EET > 14,15-EET > 8,9-EET >> 5,6-EET (Capdevila et al., 2000). Also, the observations made by Bylund et al. (1998) that CYP3A1 could mediate midchain hydroxylation based on immunoinhibition data were confirmed by our results that mHETEs are the major metabolites for CYP3A1. In previously published studies, CYP2A1-mediated formation of EETs and 19- and 20-HETE could not be detected (c.f. other CYP2 enzymes), and this finding is consistent with our finding that CYP2A1 has the lowest AA-metabolizing activity among the tested enzymes (Imaoka et al., 2005).

Several P450 enzymes can mediate the metabolism of AA; however, the contribution of each of these enzymes to overall AA metabolism has to be varied significantly. P450 expression and their catalytic activities are the two factors that dictate the contribution of a P450 enzyme to AA metabolism in a tissue. With respect to P450

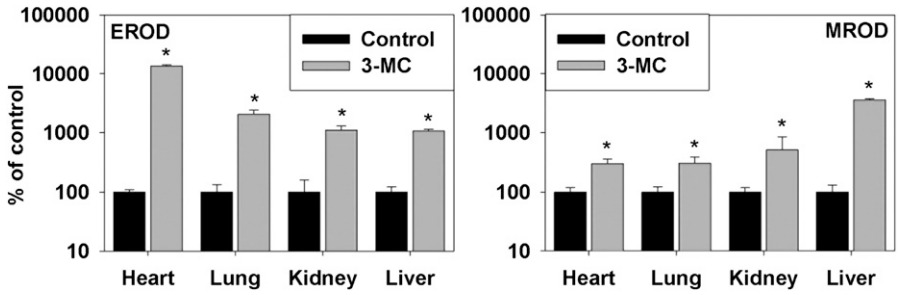

Fig. 6. The effect of 3-MC treatment on CYP1A1 and CYP1A2 activity of rat heart, lung, kidney, and liver microsomes. Microsomal protein of the heart, lungs, kidneys, or liver was incubated with EROD or MROD for 30 minutes as described under *Materials and Methods*. Fluorescence associated with resorufin formation was measured at excitation and emission wavelengths of 535 and 585 nm Results are presented as mean and S.E. (n = 4). *Difference was significant at $P < 0.05$.

expression, substantial differences have been reported between different tissues and organs (Zordoky et al., 2008; El-Sherbeni et al., 2013). Additionally, AA-metabolizing activity demonstrated great variation among P450 enzymes. Normally, highly expressed P450 enzymes with high activity will have a greater contribution to AA metabolism than a low-expressed or low-activity P450 enzyme. Apparently, CYP1As and CYP2Cs have a substantial role in AA metabolism as a result of their high AA-metabolizing activity. Also, it has been reported that CYP1As are constitutively expressed in different rat organs, including the heart, lungs, kidneys, and liver. CYP1A activity is remarkably higher in the liver compared with the heart, lungs, and kidneys (Elsherbiny et al., 2010). This is in line with our results that the liver has the highest formation rate of CYP1As major metabolites, ω-1→4 HETEs, and the heart has the lowest rate. The expression of CYP2Cs has been reported to be the highest in the liver, followed by the kidneys, and it is lowest in the heart and lungs (El-Sherbeni et al., 2013). This finding correlates with the rate of EETs formation, which is highest in the liver, followed by kidneys, then the heart and lungs. A noteworthy finding was that the liver has the highest formation rate of all groups of P450-AA metabolites, which is consistent with the fact that liver has the highest P450 content among the body organs. Being an important P450-metabolizing enzyme in mammals (Martignoni et al., 2006), CYP2E1 has been considered a major ω-1→4 AA hydroxylase. However, experimentally, CYP2E1 contribution to the constitutive formation of ω-1→4 HETEs has been reported to be minor (Laethem et al., 1993; Capdevila et al., 2000; Poloyac et al., 2004). This contradiction is explainable by our results that CYP2E1 has one of the lowest AA-metabolizing activities among the tested P450 enzymes.

In the current study, CYP1A1-, CYP1A2-, CYP2C6-, and CYP2C11-mediated AA metabolism was determined to follow substrate inhibition kinetics. Using this atypical model to describe enzyme activity allows more accurate estimation of kinetic parameters values (Houston and Kenworthy, 2000). The mechanism by which the excess substrate can inhibit the activity of an enzyme is not fully elucidated (Lin et al.,

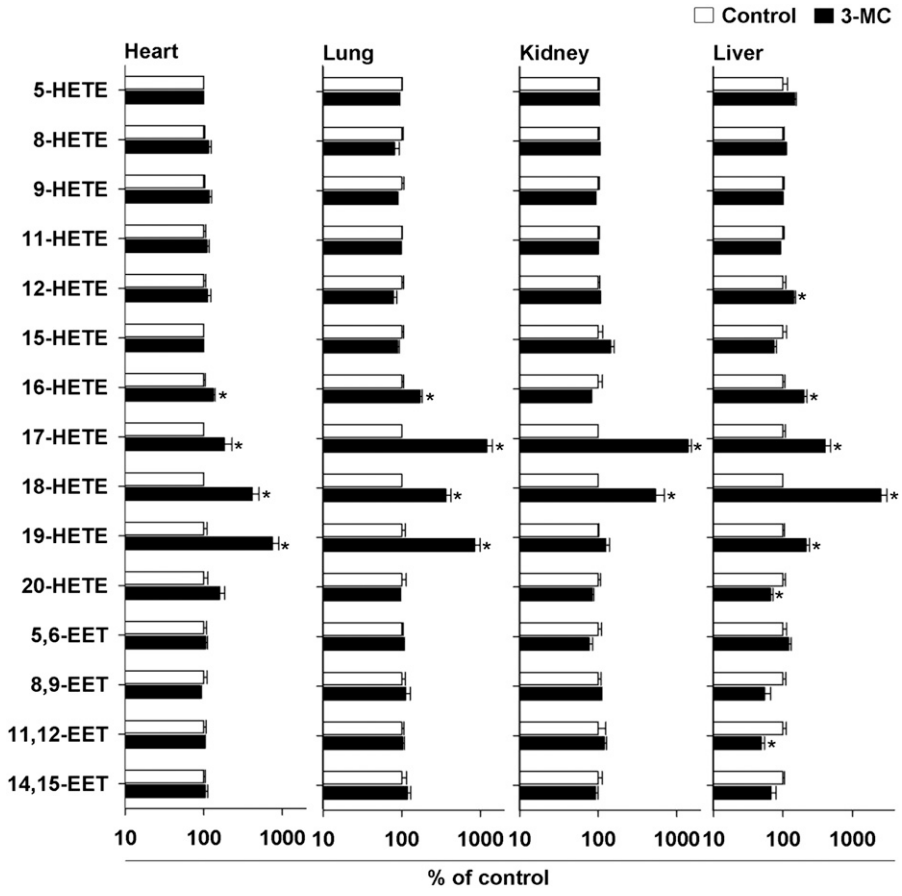

Fig. 7. The effect of 3-MC treatment on AA metabolism by rat heart, lung, kidney, and liver microsomes. Microsomal protein of the heart, lungs, kidneys, or liver was incubated with AA for 30 minutes as described under *Materials and Methods*. AA metabolites were measured by liquid chromatography-electrospray ionization-mass spectrometry as described in *Materials and Methods*. The amounts of undetectable metabolites in control samples were assumed to be 0.05 ng (the lowest lower limit of quantitation) per injection volume. Results are presented as mean and S.E. (n = 4). *Difference was significant at $P < 0.05$.

2001). Probably, the decrease in enzyme activity can be attributed to reaction products themselves (Lin et al., 2001). In agreement with our results, Xu et al. (2004) reported that CYP4F1- and CYP4F4-mediated ω-hydroxylation of AA follows substrate inhibition kinetics. The phenomenon of substrate inhibition has been reported to have regulatory role in several metabolic pathways (Reed et al., 2010).

P450-AA metabolites have multifaceted roles in the regulation of several biologic functions. Interestingly, the reported experimental effects of P450 modulations on biologic systems can be explainable in light of P450 AA-metabolizing activities. Considering that EETs and ω-1→4 HETEs are more cytoprotective, whereas mHETEs and 20-HETE are more cytotoxic, we suggest that CYP1A1, CYP1A2, and CYP2C11 play cytoprotective roles in biologic systems. In this context, it has been previously reported that the induction of CYP2C11 protects rats from ischemic brain injury (Alkayed et al., 2002; Liu and Alkayed, 2005), which is explainable by the predominant role of CYP2Cs in the formation of EETs in vivo (El-Sherbeni et al., 2013). Also, consistent with our explanation, an increase in blood pressure has been reported in CYP1A1-knockout mice (Agbor et al., 2012). Moreover, cardiac hypertrophy has been reported in aryl hydrocarbon-receptor knockout mice, which show decreased levels of CYP1A1 and CYP1A2 (Lund et al., 2003), whereas CYP1A1 and CYP1A2 induction was reported to protect rats from hyperoxic pulmonary toxicity, knocking out CYP1A1 and CYP1A2 increased pulmonary toxicity in mice (Couroucli et al., 2002; Jiang et al., 2004). Also, liver fibrosis was reported to be increased in aryl hydrocarbon-receptor knockout mice (Fernandez-Salguero et al., 1995; Peterson et al., 2000). On the other hand, the observed low AA-metabolizing activity of CYP2E1 and CYP3A1 can explain, at least in part, why CYP2E1- and CYP3A-knockout mice did not show any physiologic abnormalities compared with wild-type mice (Lee et al., 1996; van Herwaarden et al., 2007).

In the current study, we determined CYP1A involvement in AA metabolism in the microsomes of the heart, lungs, kidneys, and liver. The effects of chemical inhibition and immunoinhibition on AA metabolism were in agreement that CYP1A is a major contributor to ω-1→4 HETEs formation in vivo as evident by recombinant CYP1A1 and CYP1A2 results. Also, the induction of CYP1A levels resulted in a remarkable increase in ω-1→4 HETE formation in all organs. Interestingly, even at the constitutive level, CYP1As contributed significantly to ω-1→4 HETE formation in the liver and, to a lesser extent, in the lungs. On the other hand, anti-CYP1As antibodies inhibited the formation of all EETs and α-NF inhibited the formation of 14,15-EET in liver, whereas the induction of CYP1As led to an inhibition of the formation of 11,12-EET in liver. These results may be due to nonselective modulation of P450 enzymes other than CYP1As. However, we cannot exclude the possibility that CYP1A2 may also play a role in the formation of AA metabolites, other than ω-1→4 HETEs, in liver. It is well known that CYP1A2 is one of the major P450 in mammalian liver (Yeung et al., 2014). Generally, inhibiting CYP1As by α-NF or by anti-CYP1As antibodies or inducing CYP1As by 3-MC is considered a valid and selective method for determining the involvement of CYP1As in the metabolism of a compound (Nakajima et al., 1992; Carlson et al., 1998; Reid et al., 1999). However, AA metabolism is mediated by several cointeracting P450 enzymes that may require the use of multiple approaches to determine the specific contribution of CYP1As to AA metabolism by comparing the results of these approaches.

In conclusion, AA metabolism mediated by P450 enzymes showed significant differences in AA-metabolizing activity and regioselectivity. Apparently, P450 enzymes can have either beneficial or harmful effects on biologic systems according to their AA metabolic profile. Our results suggest that CYP1As and CYP2C11 would have beneficial effects since CYP1As are the predominant ω-1→4 AA-hydroxylases, whereas CYP2C11 is the predominant AA epoxygenase. Furthermore, it seems that AA metabolism is dominated by a relatively small group of P450s; therefore, altering certain metabolites by the pharmacologic modulation of a single P450 is feasible. Our results suggest that CYP1A1 and CYP1A2 are of great importance because of their inducibility and their significant contribution to AA metabolism. However, further investigation is needed to determine the potential beneficial effects of pharmacologic modulation of CYP1A1 and CYP1A2 enzymes in vivo. Our results link alterations in P450 expression to pathologic and physiologic changes in tissues levels of P450-derived AA metabolites, thus presenting protein targets for pharmacologic modulation.

Acknowledgments

The authors thank Dr. Vishwa Somayaji for excellent technical assistance with liquid chromatography-electrospray ionization-mass spectrometry.

Authorship Contributions

Participated in research design: El-Sherbeni, El-Kadi.
Conducted experiments: El-Sherbeni.
Performed data analysis: El-Sherbeni, El-Kadi.
Wrote or contributed to the writing of the manuscript: El-Sherbeni, El-Kadi.

References

Agbor LN, Walsh MT, Boberg JR, and Walker MK (2012) Elevated blood pressure in cytochrome P4501A1 knockout mice is associated with reduced vasodilation to omega-3 polyunsaturated fatty acids. *Toxicol Appl Pharmacol* **264**:351–360.
Alkayed NJ, Goyagi T, Joh HD, Klaus J, Harder DR, Traystman RJ, and Hurn PD (2002) Neuroprotection and P450 2C11 upregulation after experimental transient ischemic attack. *Stroke* **33**:1677–1684.
Alonso-Galicia M, Falck JR, Reddy KM, and Roman RJ (1999) 20-HETE agonists and antagonists in the renal circulation. *Am J Physiol* **277**:F790–F796.
Barakat MM, El-Kadi AO, and du Souich P (2001) L-NAME prevents in vivo the inactivation but not the down-regulation of hepatic cytochrome P450 caused by an acute inflammatory reaction. *Life Sci* **69**:1559–1571.
Bednar MM, Gross CE, Balazy MK, Belosludtsev Y, Colella DT, Falck JR, and Balazy M (2000) 16(R)-hydroxy-5,8,11,14-eicosatetraenoic acid, a new arachidonate metabolite in human polymorphonuclear leukocytes. *Biochem Pharmacol* **60**:447–455.
Benassayag C, Mignot TM, Haourigui M, Civel C, Hassid J, Carbonne B, Nunez EA, and Ferre F (1997) High polyunsaturated fatty acid, thromboxane A2, and alpha-fetoprotein concentrations at the human feto-maternal interface. *J Lipid Res* **38**:276–286.
Blewett AJ, Varma D, Gilles T, Libonati JR, and Jansen SA (2008) Development and validation of a high-performance liquid chromatography-electrospray mass spectrometry method for the simultaneous determination of 23 eicosanoids. *J Pharm Biomed Anal* **46**:653–662.
Brash AR (2001) Arachidonic acid as a bioactive molecule. *J Clin Invest* **107**:1339–1345.
Bylund J, Kunz T, Valmsen K, and Oliw EH (1998) Cytochromes P450 with bisallylic hydroxylation activity on arachidonic and linoleic acids studied with human recombinant enzymes and with human and rat liver microsomes. *J Pharmacol Exp Ther* **284**:51–60.
Capdevila JH (2007) Regulation of ion transport and blood pressure by cytochrome p450 monooxygenases. *Curr Opin Nephrol Hypertens* **16**:465–470.
Capdevila JH, Falck JR, and Harris RC (2000) Cytochrome P450 and arachidonic acid bioactivation. Molecular and functional properties of the arachidonate monooxygenase. *J Lipid Res* **41**:163–181.
Carlson GP, Hynes DE, and Mantick NA (1998) Effects of inhibitors of CYP1A and CYP2B on styrene metabolism in mouse liver and lung microsomes. *Toxicol Lett* **98**:131–137.
Carroll MA, Balazy M, Huang DD, Rybalova S, Falck JR, and McGiff JC (1997) Cytochrome P450-derived renal HETEs: storage and release. *Kidney Int* **51**:1696–1702.
Choudhary D, Jansson I, Stoilov I, Sarfarazi M, and Schenkman JB (2004) Metabolism of retinoids and arachidonic acid by human and mouse cytochrome P450 1b1. *Drug Metab Dispos* **32**:840–847.
Couroucli XI, Welty SE, Geske RS, and Moorthy B (2002) Regulation of pulmonary and hepatic cytochrome P4501A expression in the rat by hyperoxia: implications for hyperoxic lung injury. *Mol Pharmacol* **61**:507–515.
Edpuganti V and Mehvar R (2013) UHPLC-MS/MS analysis of arachidonic acid and 10 of its major cytochrome P450 metabolites as free acids in rat livers: Effects of hepatic ischemia. *J Chromatogr B Analyt Technol Biomed Life Sci* 964:153–163.
El-Sherbeni AA, Aboutabl ME, Zordoky BN, Anwar-Mohamed A, and El-Kadi AO (2013) Determination of the dominant arachidonic acid cytochrome p450 monooxygenases in rat heart, lung, kidney, and liver: protein expression and metabolite kinetics. *AAPS J* **15**:112–122.
Elsherbiny ME, El-Kadi AO, and Brocks DR (2010) The effect of beta-naphthoflavone on the metabolism of amiodarone by hepatic and extra-hepatic microsomes. *Toxicol Lett* **195**:147–154.
Fernandez-Salguero P, Pineau T, Hilbert DM, McPhail T, Lee SS, Kimura S, Nebert DW, Rudikoff S, Ward JM, and Gonzalez FJ (1995) Immune system impairment and hepatic fibrosis in mice lacking the dioxin-binding Ah receptor. *Science* **268**:722–726.
Hammarström S, Hamberg M, Samuelsson B, Duell EA, Stawiski M, and Voorhees JJ (1975) Increased concentrations of nonesterified arachidonic acid, 12L-hydroxy-5,8,10,14-eicosatetraenoic

acid, prostaglandin E2, and prostaglandin F2alpha in epidermis of psoriasis. *Proc Natl Acad Sci USA* **72**:5130–5134.
Holla VR, Makita K, Zaphiropoulos PG, and Capdevila JH (1999) The kidney cytochrome P-450 2C23 arachidonic acid epoxygenase is upregulated during dietary salt loading. *J Clin Invest* **104**:751–760.
Houston JB and Kenworthy KE (2000) In vitro-in vivo scaling of CYP kinetic data not consistent with the classical Michaelis-Menten model. *Drug Metab Dispos* **28**:246–254.
Iliff JJ, Jia J, Nelson J, Goyagi T, Klaus J, and Alkayed NJ (2010) Epoxyeicosanoid signaling in CNS function and disease. *Prostaglandins Other Lipid Mediat* **91**:68–84.
Imaoka S, Hashizume T, and Funae Y (2005) Localization of rat cytochrome P450 in various tissues and comparison of arachidonic acid metabolism by rat P450 with that by human P450 orthologs. *Drug Metab Pharmacokinet* **20**:478–484.
Imig JD (2012) Epoxides and soluble epoxide hydrolase in cardiovascular physiology. *Physiol Rev* **92**:101–130.
Jiang W, Welty SE, Couroucli XI, Barrios R, Kondraganti SR, Muthiah K, Yu L, Avery SE, and Moorthy B (2004) Disruption of the Ah receptor gene alters the susceptibility of mice to oxygen-mediated regulation of pulmonary and hepatic cytochromes P4501A expression and exacerbates hyperoxic lung injury. *J Pharmacol Exp Ther* **310**:512–519.
Kapelyukh Y, Paine MJ, Maréchal JD, Sutcliffe MJ, Wolf CR, and Roberts GC (2008) Multiple substrate binding by cytochrome P450 3A4: estimation of the number of bound substrate molecules. *Drug Metab Dispos* **36**:2136–2144.
Kayama Y, Minamino T, Toko H, Sakamoto M, Shimizu I, Takahashi H, Okada S, Tateno K, Moriya J, and Yokoyama M, et al. (2009) Cardiac 12/15 lipoxygenase-induced inflammation is involved in heart failure. *J Exp Med* **206**:1565–1574.
Kiss L, Schütte H, Mayer K, Grimm H, Padberg W, Seeger W, and Grimminger F (2000) Synthesis of arachidonic acid-derived lipoxygenase and cytochrome P450 products in the intact human lung vasculature. *Am J Respir Crit Care Med* **161**:1917–1923.
Kramer MA and Tracy TS (2008) Studying cytochrome P450 kinetics in drug metabolism. *Expert Opin Drug Metab Toxicol* **4**:591–603.
Laethem RM, Balazy M, Falck JR, Laethem CL, and Koop DR (1993) Formation of 19(S)-, 19 (R)-, and 18(R)-hydroxyeicosatetraenoic acids by alcohol-inducible cytochrome P450 2E1. *J Biol Chem* **268**:12912–12918.
Lee SS, Buters JT, Pineau T, Fernandez-Salguero P, and Gonzalez FJ (1996) Role of CYP2E1 in the hepatotoxicity of acetaminophen. *J Biol Chem* **271**:12063–12067.
LiCata VJ and Allewell NM (1997) Is substrate inhibition a consequence of allostery in aspartate transcarbamylase? *Biophys Chem* **64**:225–234.
Lin Y, Lu P, Tang C, Mei Q, Sandig G, Rodrigues AD, Rushmore TH, and Shou M (2001) Substrate inhibition kinetics for cytochrome P450-catalyzed reactions. *Drug Metab Dispos* **29**: 368–374.
Liu M and Alkayed NJ (2005) Hypoxic preconditioning and tolerance via hypoxia inducible factor (HIF) 1alpha-linked induction of P450 2C11 epoxygenase in astrocytes. *J Cereb Blood Flow Metab* **25**:939–948.
Lowry OH, Rosebrough NJ, Farr AL, and Randall RJ (1951) Protein measurement with the Folin phenol reagent. *J Biol Chem* **193**:265–275.
Lund AK, Goens MB, Kanagy NL, and Walker MK (2003) Cardiac hypertrophy in aryl hydrocarbon receptor null mice is correlated with elevated angiotensin II, endothelin-1, and mean arterial blood pressure. *Toxicol Appl Pharmacol* **193**:177–187.
Martignoni M, Groothuis GM, and de Kanter R (2006) Species differences between mouse, rat, dog, monkey and human CYP-mediated drug metabolism, inhibition and induction. *Expert Opin Drug Metab Toxicol* **2**:875–894.
Morisseau C (2013) Role of epoxide hydrolases in lipid metabolism. *Biochimie* **95**:91–95.
Nakajima T, Wang RS, Elovaara E, Park SS, Gelboin HV, and Vainio H (1992) A comparative study on the contribution of cytochrome P450 isozymes to metabolism of benzene, toluene and trichloroethylene in rat liver. *Biochem Pharmacol* **43**:251–257.
Norris PC, Reichart D, Dumlao DS, Glass CK, and Dennis EA (2011) Specificity of eicosanoid production depends on the TLR-4-stimulated macrophage phenotype. *J Leukoc Biol* **90**:563–574.
Peterson TC, Hodgson P, Fernandez-Salguero P, Neumeister M, and Gonzalez FJ (2000) Hepatic fibrosis and cytochrome P450: experimental models of fibrosis compared to AHR knockout mice. *Hepatol Res* **17**:112–125.
Poloyac SM, Tortorici MA, Przychodzin DI, Reynolds RB, Xie W, Frye RF, and Zemaitis MA (2004) The effect of isoniazid on CYP2E1- and CYP4A-mediated hydroxylation of arachidonic acid in the rat liver and kidney. *Drug Metab Dispos* **32**:727–733.
Reddy MA, Thimmalapura PR, Lanting L, Nadler JL, Fatima S, and Natarajan R (2002) The oxidized lipid and lipoxygenase product 12(S)-hydroxyeicosatetraenoic acid induces hypertrophy and fibronectin transcription in vascular smooth muscle cells via p38 MAPK and cAMP response element-binding protein activation. Mediation of angiotensin II effects. *J Biol Chem* **277**:9920–9928.
Reed MC, Lieb A, and Nijhout HF (2010) The biological significance of substrate inhibition: a mechanism with diverse functions. *BioEssays* **32**:422–429.
Reid JM, Kuffel MJ, Miller JK, Rios R, and Ames MM (1999) Metabolic activation of dacarbazine by human cytochromes P450: the role of CYP1A1, CYP1A2, and CYP2E1. *Clin Cancer Res* **5**: 2192–2197.
Roman RJ (2002) P-450 metabolites of arachidonic acid in the control of cardiovascular function. *Physiol Rev* **82**:131–185.
Roman RJ, Maier KG, Sun CW, Harder DR, and Alonso-Galicia M (2000) Renal and cardiovascular actions of 20-hydroxyeicosatetraenoic acid and epoxyeicosatrienoic acids. *Clin Exp Pharmacol Physiol* **27**:855–865.
Schwarz D, Kisselev P, Ericksen SS, Szklarz GD, Chernogolov A, Honeck H, Schunck WH, and Roots I (2004) Arachidonic and eicosapentaenoic acid metabolism by human CYP1A1: highly stereoselective formation of 17(R),18(S)-epoxyeicosatetraenoic acid. *Biochem Pharmacol* **67**:1445–1457.
Stec DE, Gannon KP, Beaird JS, and Drummond HA (2007) 20-Hydroxyeicosatetraenoic acid (20-HETE) stimulates migration of vascular smooth muscle cells. *Cell Physiol Biochem* **19**: 121–128.
van Herwaarden AE, Wagenaar E, van der Kruijssen CM, van Waterschoot RA, Smit JW, Song JY, van der Valk MA, van Tellingen O, van der Hoorn JW, and Rosing H, et al. (2007) Knockout of cytochrome P450 3A yields new mouse models for understanding xenobiotic metabolism. *J Clin Invest* **117**:3583–3592.
Xu F, Falck JR, Ortiz de Montellano PR, and Kroetz DL (2004) Catalytic activity and isoform-specific inhibition of rat cytochrome p450 4F enzymes. *J Pharmacol Exp Ther* **308**:887–895.
Yeung CK, Shen DD, Thummel KE, and Himmelfarb J (2014) Effects of chronic kidney disease and uremia on hepatic drug metabolism and transport. *Kidney Int* **85**:522–528.
Zhang F, Deng H, Kemp R, Singh H, Gopal VR, Falck JR, Laniado-Schwartzman M, and Nasjletti A (2005) Decreased levels of cytochrome P450 2E1-derived eicosanoids sensitize renal arteries to constrictor agonists in spontaneously hypertensive rats. *Hypertension* **45**:103–108.
Zordoky BN, Aboutabl ME, and El-Kadi AO (2008) Modulation of cytochrome P450 gene expression and arachidonic acid metabolism during isoproterenol-induced cardiac hypertrophy in rats. *Drug Metab Dispos* **36**:2277–2286.
Zou AP, Fleming JT, Falck JR, Jacobs ER, Gebremedhin D, Harder DR, and Roman RJ (1996) 20-HETE is an endogenous inhibitor of the large-conductance Ca(2+)-activated K+ channel in renal arterioles. *Am J Physiol* **270**:R228–R237.

Address correspondence to: Dr. Ayman O.S. El-Kadi, Faculty of Pharmacy and Pharmaceutical Sciences, 2142J Katz Group-Rexall Centre for Pharmacy and Health Research, University of Alberta, Edmonton, AB, Canada T6G 2E1. E-mail: aelkadi@ualberta.ca